Electrical Properties of $PbTiO_3$ Thin Film Diode

Chaw Loon Thu[1], Pwint Yee Thein[2], Than Than Win[1], Yin Maung Maung[1], Ko Ko Kyaw Soe[1]

[1]*Department of Physics, University of Yangon, Myanmar*

[2] *Department of Physics, Nationalities Youth Resource Development Degree College, Yangon, Myanmar*

chawloon.thu@gmail.com

***Abstract* – Lead titanate ($PbTiO_3$) powder was prepared by starting chemicals of lead nitrate ($Pb(NO_3)_2$), potassium hydroxide (KOH) and different amount of titanium dioxide (TiO_2) by classical hydrothermal sysnthesis at low temperature. X-ray Diffraction (XRD) technique was used to examine the phase identification and crystallographic properties of $PbTiO_3$ powder. Hydrothermal $PbTiO_3$ thin film was fabricated on the SiO_2/Si substrate by using Single Wafer Spin Processor (MODEL WS-400BZ-6NPP/LITE). Scanning Electron Microscopy (SEM) was employed to study the grain morphology and film thickness. Electrical properties of $PbTiO_3/SiO_2$/Si cell were measured by means of I-V characteristics.**

***Keywords* - Hydrothermal synthesis, thin film, SEM analysis, I-V characteristics**

I. INTRODUCTION

Ferroelectric ceramics have been in the areas such as dielectric ceramics for capacitor applications, ferroelectric thin films for non-volatile memories, piezoelectric materials for medical ultrasound imaging and actuators and electro-optic materials for data storage and displays. With the development of ceramic processing and thin film technology, many new applications have emerged [1]. Ferroelectric materials can be used in different ways in memory designs [2].The common and defining feature of all ferroelectrics is the presence of a field re-orientable spontaneous polarization [3].

Lead titanate $PbTiO_3$ type ferroelectric thin films have also been demanded for application to many kinds of electric devices including sensors, capacitors and microactuators [4]. Lead titanate, $PbTiO_3$ (PT) is a well-known ferroelectric and piezoelectric material. It has many important technological applications in electronics and microelectronics, because of its high Curie temperature, high pyroelectric coefficient and high spontaneous polarization. Several methods have been employed to prepare $PbTiO_3$ powders in the literature, including cherqcal coprecipitation, sol-gel, and hydrothermal reaction [5].

Hydrothermal synthesis is a promising method that involves crystallization in aqueous medium at elevated temperatures for the manufacture of advanced ceramic powders and thin films. Lead titanate $PbTiO_3$ ceramics have been made by hydrothermal method using a wide variety of precursors, processing temperature, and mineraliza [6]. The hydrothermal method is in attractive technique for formation of perovskite type ceramic [7].

In the present work, hydrothermal synthesis PT thin films were fabricated on SiO_2/Si substrates. Due to the effect of different TiO_2 contents, the microstructural properties and I-V characteristics of all PT films were investigated.

II. EXPERIMENTAL PROCEDURE

By using the hydrothermal versatile technique, $PbTiO_3$ ceramic powder was produced. The powder was grown by reacting fixed amount of lead (II) nitrate ($Pb(NO_3)_2$) with different contents of TiO_2 in alkaline aqueous solution of 15 ml KOH at 110-200°C in teflon-lined stainless steel vessel. Firstly, 1mol of KOH pellet was added to1liter of deionized water (DIW) and slowly stirred for homogeneous solution. Then 1g of $Pb(NO_3)_2$, prepared hydrated KOH solution and different amounts of TiO_2 ranging 0.2g to 0.26g were mixed in Teflon-lined stainless steel vessel, as shown in Fig.1. The mixture was oven-dried at 200°C for 6h in the Teflon-lined stainless steel vessel at sealed condition and then naturally cooled down at room temperature. In this way, $PbTiO_3$ powder with different TiO_2 contents was successfully formed.

Clean Si substrate was heated at 1200°C to form the SiO_2 intermediate layer. $PbTiO_3$ powder with different TiO_2 contents were separately mixed with 1.5 ml of ethylene glycol and 3 drops of 2-methoxyethanol to obtain $PbTiO_3$ sol solutions. After receiving PT colloidal solutions, they were coated on SiO_2/Si substrate by using Single Wafer Spin Processor (MODEL WS-400BZ 6NPP/ LITE), as shown in Fig.2. The operation conditions were shown in Table I. SiO_2/Si substrate was placed on Fragment Adapter and the solution was poured onto SiO_2/Si substrate with constant rate of 2000 rpm at spin time interval of 2 min. After fabrication, all fabricated PT films were annealed at 500ºC for 1 h. X-ray diffraction (XRD) and Scanning Electron Microscopy (SEM) were used to characterize the samples.

TABLE I
OPERATION CONDITIONS

Spin speed	2000rpm
Spin time	2 min
N_2 gas pressure	60 psi
Vacuum	25.3 (inches of Hg)

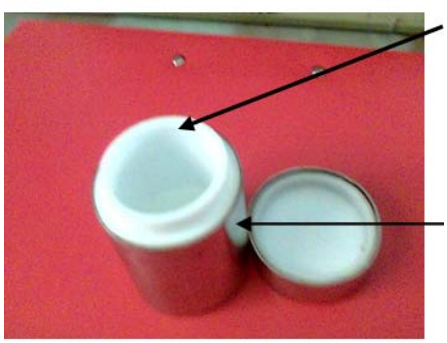

Fig. 1 Teflon-lined stainless steel vessel

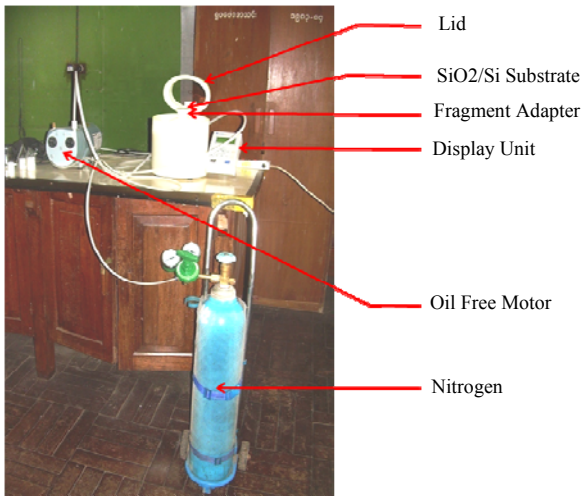

Fig. 2 Single Wafer Spin Processor
(MODEL WS-400BZ- 6NPP-LITE)

III. RESULTS AND DISCUSSION

A. XRD Analysis

X- ray diffraction XRD is a non-destructive technique for the qualitative and quantitative analysis of the crystalline materials, in the form of powder or solid. The information about the crystallographic properties such as crystallite size and lattice parameters of all samples has been obtained from the XRD profiles. The XRD pattern of hydrothermal synthesized $PbTiO_3$ specimens was shown in Fig. 3 (a - d).

As shown in Fig. 3 (a), the upper and lower sites of the graph were represented the XRD pattern of product PT powder (TiO_2 0.2 g) (sample1) and standard powder respectively. Ten reflections of the standard peaks were scanned within the diffraction angles range from 10° to 70°. As it was displayed in the spectrum, nine reflections were formed. Seven reflections of the $PbTiO_3$ PT (1) powder were consistent with that of standard PT (1) powder.

The strongest peak was (101) plane at 2θ= 29.40°. It was a little left shifted as compared with that of standard. The XRD pattern of PT (2) was shown in Fig. 3 (b). The sample exhibited the most dominant peak at 2θ=30°. The XRD profile of $PbTiO_3$ (3) powder was shown in Fig. 3 (c). According to the spectrum, the most intense peak (101) was formed at 29. 40° and it was equal to that of the PT (1). The most intense peak of $PbTiO_3$ (3) powder was formed at the same diffraction angle of the standard powder. They were absolutely well matched. There were 10 reflections on the standard powder ranging diffraction angle 2θ from 10° to 70°. The XRD profile of PT (4) powder showed that all reflections were well-matched with those of the standard powder.

The maximum degree of the crystallite size was found to be TiO_2 content of 0.24 g (Sample 3). According the XRD spectrum, $PbTiO_3$ was formed with tetragonal symmetry within the detection limit of XRD machine (RIGAKU Multiflex (Japan) X-ray diffractometre, Cu-K_α=1.54056Å radiation). The lattice constants (a and c) and lattice distortion (c/a) were calculated and listed in Table II. The dominant peak (crystal plane), peak position and relative intensity were collected and listed in Table III. The crystallite size derived from Debye-Scherrer formula was quoted in Table IV. The largest value of crystallite size was found at $PbTiO_3$ with 0.22 g of TiO_2 content. The structure of this specimen led to relatively high crystallinity.

TABLE II
THE LATTICE CONSTANTS (A AND C) AND LATTICE DISTORTION (C/A) OF $PBTIO_3$ POWDERS

$PbTiO_3$	Ti content (g)	Dominant peak	Lattice parameter a(Å)	Lattice parameter c(Å)	Tetragonally c/a
Sample1	0.20	(101)	3.91	4.83	1.23
Sample 2	0.22	(101)	3.90	4.39	1.12
Sample 3	0.24	(101)	3.90	4.83	1.23
Sample 4	0.26	(101)	3.88	4.81	1.23

TABLE III
DOMINANT PEAK, PEAK POSITION AND RELATIVE INTENSITY OF $PBTIO_3$ POWDER

TiO_2 constant in PT	Crystal plane	Peak position (deg)	Intensity (cps)
Sample 1	(101)	29.40	504
Sample 2	(101)	30	1613
Sample 3	(101)	29.40	419
Sample 4	(101)	29.60	320

TABLE IV
CRYSTALLITE SIZE OF PBTIO$_3$ POWDER

$PbTiO_3$	Crystallite size(nm)
Sample 1	27.9
Sample 2	53.8
Sample 3	14.8
Sample 4	17.0

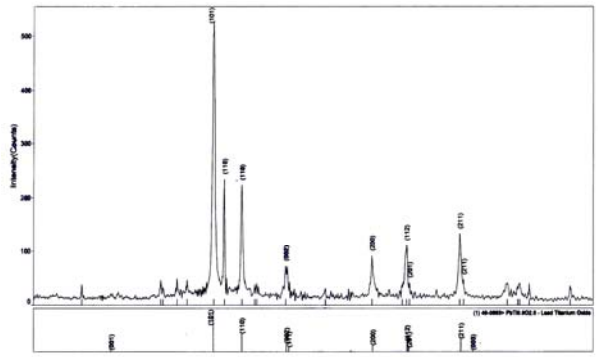

Fig. 3 (a) XRD analysis of $PbTiO_3$ powder with 0.2g of TiO_2 content

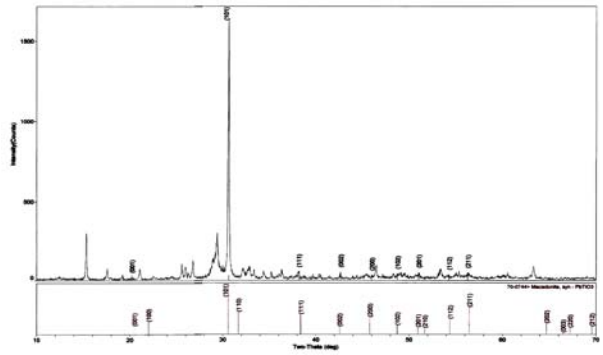

Fig. 3 (b) XRD analysis of $PbTiO_3$ powder with 0.22g of TiO_2 content

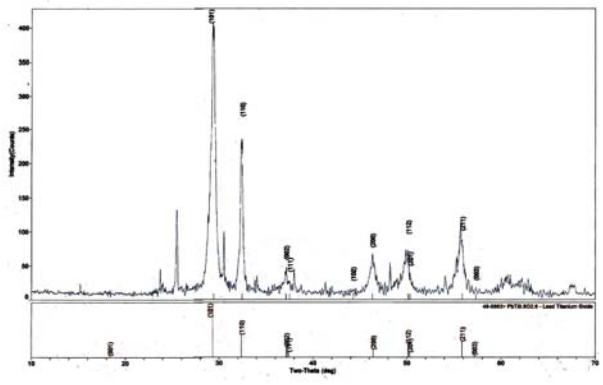

Fig. 3 (c) XRD analysis of PbTiO3 powder with 0.24g of TiO2 content

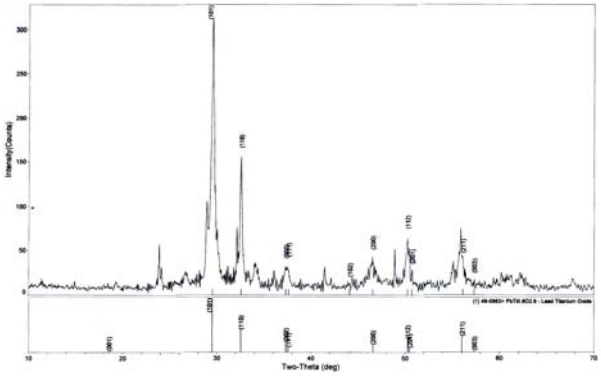

Fig. 3 (d) XRD analysis of $PbTiO_3$ powder with 0.26g of TiO_2 content

B. SEM Analysis

The SEM images of $PbTiO_3$ films with different TiO_2 contents were shown in Fig. 4 (a - d). All SEM images were significantly different in morphology. Fig. 4 (a) showed that grain growth was irregular indicating some impurities formation during thermal treatment. The microstructure of $PbTiO_3$ film with 0.22g TiO_2 content was shown in Fig. 4 (b). The microstructure showed clearly that the grain distribution was non-uniform. The grain size was also non-uniform and ranged from 0.028 μm to 1.02 μm.

Some micro-cracks were formed and it might be due to the large viscosity level of $PbTiO_3$ sol solution. The sample had flaky surface. Some porosities were formed and some grains were separately distributed by pores. Agglomeration was formed on the centre of SEM micrograph. Fig. 4 (c) indicated the SEM microphotograph $PbTiO_3$ film with 0.24g TiO_2 content. The graph was flat and grain was tightly packed. The size of product grain was ranged from 0.29 to 0.76 μm. The surface morphology did not show crack and the shape of grain was sphere. Some grains were separated by pores while others were distributed in continuity. SEM image showed no agglomeration indicating the $PbTiO_3$ sol solution was optimal quality. Fig. 4 (d) was SEM morphology of $PbTiO_3$ film with 0.26g TiO_2 content. It was obvious that the surface morphology was almost homogeneous. It was composed of regular and sphere grains with sizes ranging from 0.32μm to 0.85μm.

Film thickness of the $PbTiO_3$ film was obtained from the cross-sectional SEM image. Fig. 5 (a - d) showed the cross-sectional SEM images of $PbTiO_3$ film on p-Si (100) substrate. The film thicknesses were 19.3μm, 22.9μm, 14.9μm and 31.7μm for respective films. The minimum value of film thickness was obtained for the $PbTiO_3$ sample with 0.24g TiO_2 content.

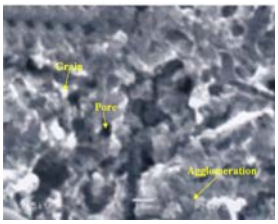

Fig. 4 (a) SEM micrograph of $PbTiO_3$ thin film at TiO_2 0.2g

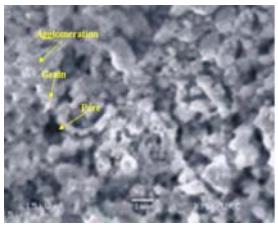

Fig. 4 (b) SEM micrograph of $PbTiO_3$ thin film at TiO_2 0.22g

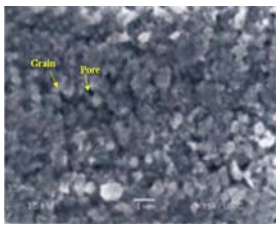

Fig. 4 (c) SEM micrograph of $PbTiO_3$ thin film at TiO_2 0.24g

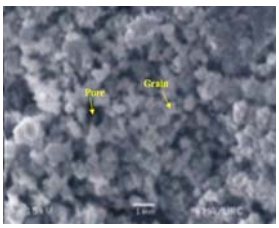

Fig. 4 (d) SEM micrograph of $PbTiO_3$ thin film at TiO_2 0.26g

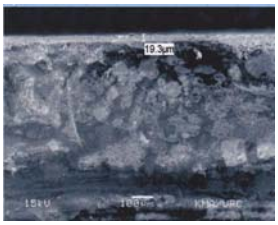

Fig. 5 (a) Cross-sectional view of $PbTiO_3$ thin film at TiO_2 0.2g

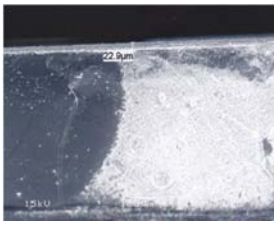

Fig. 5 (b) Cross-sectional view of $PbTiO_3$ thin film at TiO_2 0.22g

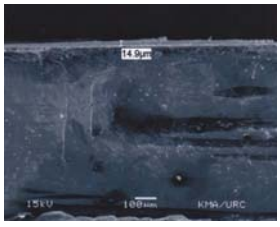

Fig. 5 (c) Cross-sectional view of $PbTiO_3$ thin film at TiO_2 0.24g

Fig. 5 (d) Cross-sectional view of $PbTiO_3$ thin film at TiO_2 0.26g

C. I-V Characteristics

I-V characteristics were measured to examine the electrical properties of Cu/PT/SiO_2/Si/Cu structure. The change in current with respect to applied voltage data was recorded and plotted at Fig. 6 (a). The I-V graph seemed to be asymmetric and gave a hint of rectification effect. On the forward bias region, the dead-space widened at about 1.6V which was the threshold voltage.

The nature of I-V graph was typical of a normal diode. Fig. 6(b) showed the ln I-V characteristic curve. The diode parameters such as ideality factor (diode quality factor, η) and zero-bias barrier height (ϕ_{b0}) were calculated. The value of η was found to be greater than unity. It might be due to the wide space charge region formed between p-n junction. The smallest value of η was obtained for the film with 0.26g TiO_2 content. The zero-bias barrier height (ϕ_{b0}) was less than unity, indicated that the TiO_2 film behaved as a typical diode.

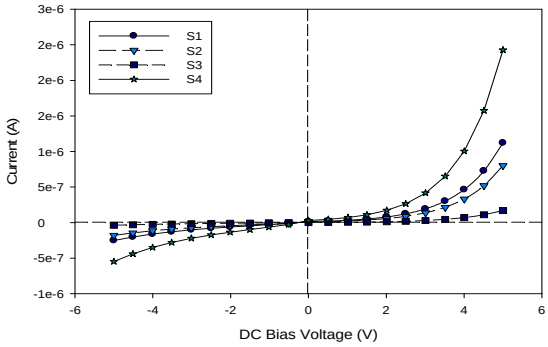

Fig. 6 (a) I-V characteristics of $PbTiO_3$ films at different TiO_2 content

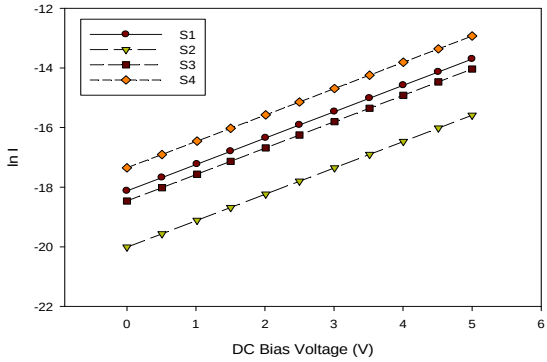

Fig. 6 (b) I-V characteristics of $PbTiO_3$ films at different TiO_2 content

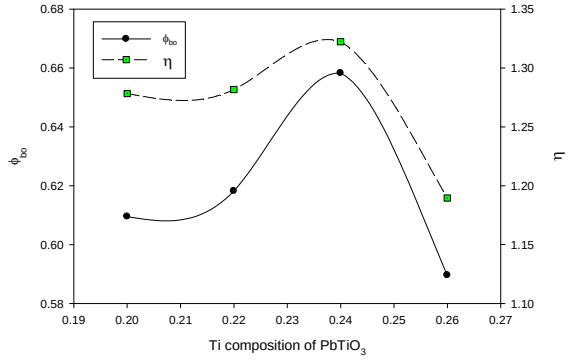

Fig. 6 (c) η and ϕ_{bo} at different Ti compositions of $PbTiO_3$ thin film

IV. CONCLUSION

From XRD result, the most intense peak (dominant peak) was formed at (101) reflection for all XRD profiles. The crystallite size was examined to be within the range of accepted value for nano-size particle. The lightest particle was caused for $PbTiO_3$ film at 0.24g (TiO_2 content). This fact revealed that sample 3 might have many contact points to react other molecules (large surface area by volume). From XRD spectrum, the maximum value of peak height for (101) dominant peak of $PbTiO_3$ film with 0.22g of TiO_2 was examined to be 1613 cps.

From SEM surface morphology investigation, altering solution chemistry was quite feasible for thin film fabrication technology. Some pores and grain growth pattern were formed and it might be due to some impurities formation during thermal treatment. The thinnest film was found at the film with 0.24g for TiO_2 content. I-V characteristics showed the rectification effect. The forward region was asymmetric with reverse region. The curve gave the trend of saturation. The ideality factor (η) was calculated to be greater than unity and it might be attributed to the leakage current. The advantages of hydrothermal synthesis were of low cost and low temperature phase transition. Moreover, it could exactly control the stoichiometry. Thus $PbTiO_3/SiO_2/Si$ laboratory-fabricated cells can be utilized for electrical appliance.

ACKNOWLEDGMENT

One of the authors, Chaw Loon Thu would like to acknowledge Pro-Reactor Dr Pho Kaung, Head of Universities' Research Centre for his kind permission to use the facilities.

REFERENCES

[1] A. Safari, et al., *Ferroelectric Ceramics: Processing, Properties & Applications*, Department of Ceramic Science and Engineering (USA: Rutgers University)

[2] W. A. Geideman, IEEE Transactions on Ultrasonics, Femoelectrics & Frequency Control vol. 38, p.704, 1991

[3] M. Daglish et al., The Institution of Professional Engineers New Zeland Transactions vol. 27, p.21, 2000

[4] T. Iijima et al., Japanese Journal of Applied Physics vol. 36, p. 5825, 1997

[5] T. Yu et al., Journal of Applied Physics vol. 93, p. 3470, 2003

[6] A. T. Chien et al., Journal of Materials Research vol. 14, p. 3303, 1999

[7] M. Cernea, Journal of Optoelectronics and Advanced Materials vol. 6, p. 1349, 2004